Eco-Friendly Synthesis of $MgO/MgAl_2O_4$ Core/Shell Nanostructures and Their Antimicrobial Evaluation Against Pathogenic Microbial Strains

Moshafi, Mohammad Hasan
Research Committee, Kerman University of Medical Sciences, Kerman, I.R. IRAN

Rajaei, Peyman
Department of Biology, Kerman Branch, Islamic Azad University, Kerman, I.R. IRAN

Ranjbar, Mehdi*[*+]*
Health in Disasters and Emergencies Research Center, Institute for Futures Studies in Health, University of Medical Sciences, Kerman, I.R. IRAN

ABSTRACT: *Nowadays antimicrobial resistance is one of the important concerns caused by the extensive use of antibiotics. Efforts to find new materials with antimicrobial effects have been more serious than before. In this study, $MgO/MgAl_2O_4$ nanoparticles were synthesized by hydrothermal technique. To investigate the physicochemical properties, scanning electron microscopy, dynamic light scattering, X-Ray Diffraction (XRD), ThermoGravimetric Analysis (TGA), and atomic force microscopy were carried out. For the purpose of evaluation of the $MgO/MgAl_2O_4$ nanoparticles, energy dispersive Scanning Electron Microscopy (SEM), Dynamic Light Scattering (DLS), TGA, Transmission Electron Microscopy (TEM), and Fourier-Transform InfraRed (FT-IR) spectroscopy ran then minimum inhibitory concentration measured on eight bacterial strains. The majority of nanoparticles were in the range of 90 to 150 nm which is the well-optimized size for our purpose. Antimicrobial analysis showed the effect of synthesized $MgO/MgAl_2O_4$ NPs on every eight microbial strains including 4-gram positive Staphylococcus epidermidis, Staphylococcus aureus, Micrococcus luteus, Bacillus subtilis and 4-gram negative strains Serratia marcesens, Escherichia coli, Pseudomonas aeruginosa, Klebsiella pneumoni.*

KEYWORDS: *Microbial resistance; Antibacterial; $MgO/MgAl_2O_4$; Eco-Friendly.*

INTRODUCTION

In the general definition of nanoparticles, particles in the range of 1 to 100 nanometers are called nanoparticles [1, 2]. These particles are designed to exhibit special and controlled properties from their raw material in normal size [3, 4], which are the result of precise control over their manufacturing process [5, 6]. Fortunately,

* *To whom correspondence should be addressed.*
+E-mail address: Mehdi.Ranjbar@kmu.ac.ir
1021-9986/2022/12/1126-1133 8/$/5.08

nanotechnology is not just a growing one-dimensional branch of science, but has kept pace with the advancement of sciences that have long existed, such as physics, chemistry, medical biology, and other sciences [7, 8]. Nanomedicine as a growing branch of nanotechnology and pharmaceuticals, with the goal of expanding drugs [9, 10] and antimicrobials [11] and imaging agents and reducing toxicity profiles is a highly active branch of science today [12, 13]. One of the most important things in drug delivery systems and pharmaceutics is to always improve drug targeting for specific cells and reduce the accumulation of drugs in cells that not only do not need them [14, 15], but sometimes the presence of drugs in those cells has potential toxic effects for that cell [16, 17]. This is often because the size of the drug molecules that are commonly used is ten times the size of a cell such as a red blood cell [18]. In this way, the drug penetrates into the cells much less than expected as a result, in order to achieve the desired goals, we will have to increase the dose or frequency of use, which in turn will cause more toxicity and create unwanted side effects [19, 20]. Nowadays, with the help of what we have available with the help of nanomedicine, pharmaceutics and treatment, we try to achieve targeted drug delivery, reduce toxicity and thus increase the efficiency of drug delivery and photography as accurately as possible. On the other hand, in the treatment of infectious diseases, bacterial resistance to newer antibiotics has always been and will be an important issue because bacterial resistance will lead to increased doses of antibiotics, increased hospital stays, increased antimicrobial therapy and ultimately increased patient mortality. Metal oxide nanoparticles due to its unique properties [21, 22], have wide applications in medical sciences such as targeted drug delivery, biomedical therapeutics, bio imaging and biosensing [23, 24]. The bacterium may be inherently resistant to a class of antibacterial agents or may become resistant to the substance by mutating the mutation or obtaining a resistance gene from other organisms [25, 26]. The use of nanotechnology by various mechanisms that have been identified so far is one of the most important methods of overcoming bacterial resistance. Metal oxide nanoparticles used as therapeutic agents in the treatment of medical diseases related to reactive oxygen species such as spinal cord repair [27], stroke and retinal degenerative disorders [28, 29]. This highlights the importance of investigating the effectiveness of the metal oxide nanoparticles (MO-NPs) on microorganisms. In this study, after fabrication and study of physicochemical properties of bismuth hydroxide and chitosan nanoparticles and fabrication of nanostructures containing these two nanoparticles, their antimicrobial effects on 8 microbial strains have been investigated and in the presence of antimicrobial effects, the lowest inhibitory concentration for the mentioned strains has been investigated.

EXPERIMENTAL SECTION

In this study, $MgO/MgAl_2O_4$ nanoparticles synthesized by hydrothermal technique [30]. To investigate the physicochemical properties, Scanning Electron Microscopy (SEM), Dynamic Light Scattering (DLS) and atomic force microscopy were evaluated. In addition, to analyze the chemical component of nanocomposites Energy Dispersive Spectroscopy (EDX), Optical properties evaluated with Shimadzu UV-2600 UV–Vis spectrophotometer and Fourier-Transform InfraRed (FT-IR) spectroscopy ran then minimum inhibitory concentration measured on seven bacterial strains.

Preparation of $MgO/MgAl_2O_4$ NPs

At the first, 0.03 g of magnesium nitrate $Mg(NO_3)_2.2H_2O$ was weighed, then 15 mL of distilled water was added to above solution under 400 rpm stirring in the reflux refrigerant system. After dissolving 0.01g Al_2O_3, the resulting solution was placed on a heater stirrer at 50 °C for 30 min and stirred at a speed of 400 rpm by a magnetic stirrer. Then 5 mL of 2 M NaOH solution was added to the resulting solution, after adding the solution containing 0.01 g of cetyltrimethylammonium bromide (CTAB) in 10 mL of deionized water, which is used as a surfactant to control the growth of nanoparticles and prevent agglomeration of nanoparticles. the mixtures were placed in Teflon container and the reactions were performed in a stainless reactor system under various conditions (Table 1), all three final mixtures were placed thermal oven for 24h.

MIC determination method

First, all strains of bacteria were prepared after 24h of culture activation. During the experiment, a new culture of bacteria was prepared every three days to monitor

Table 1: Different synthesis conditions of $MgO/MgAl_2O_4$ NPs

Sample	CTAB (g)	pH	Temperature (°C)	Time (h)	Morphology
S1	0.01	7.8-8	150	6	Sphere-like nanostructures
S2	0.01	7.8-8	180	6	Sphere-like nanostructures
S3	0.01	7.8-8	200	6	Sphere-like nanostructures
S4	0.01	7.8-8	210	6	Agglomeration

antimicrobial effects of the bacteria in their logarithmic phase. Each of the as-synthesized samples added into a balloon, then dissolve with the least amount of solvent dimethyl sulfoxide to obtain a storage concentration of 1280 μg/mL. Then 8 small sterilized tubes were removed and 2 mL of Müller Hinton broth was poured into each. Then 2 mL of the stock solution was added to the first tube and after mixing, 2 mL of the first tube was removed again and added to the second tube. this process continued until 2 mL is finally discarded from the last tube. Thus, 8 consecutive dilutions are obtained from the sample and concentrations of 0.25, 0.5, 1, 2, 4, 8, 16, 32 and 64 μg/mL are prepared. For the preparation of the culture medium, we used Müller Hinton agar. The characteristics of the bacteria used in the study are given in Table 2. Bacteria cultured 24 h before were made into a microbial suspension in the remaining 7 liquid tubes containing 2 mL of Müller-Hinton broth culture medium, which was similar in turbidity to McFarland 0.5 solution. After the first microbial test, due to the observation of good inhibitory effects of nanoparticles on bacteria, 4 concentrations were added to the tested concentrations for more accurate reporting. In this way, 11.4 g of Müller Hinton agar was weighed from the next time and reached a volume of 300 mL with distilled water and indirect heat, and the dilution operation was performed from 1 to 12 tubes. Thus, the minimum inhibitory concentration in plates containing 0.25, 0.5, 1, 2, 4, 8, 16, 32, 64 μg/mL was investigated.

RESULTS AND DISCUSSION

X-ray pattern was taken from the sample to the investigation of the purity and determine the phase structures, The X-ray diffraction pattern shows that the nanostructures are synthesized with a unique crystalline structure and a high percentage of purity. Using *Debbie Scherer's* equation, the particle size can be calculated using Equation 1 approximately:

$$D_c=K_\lambda/\beta.\cos\theta \quad (1)$$

Where in this equation θ defined as the scattering angle of X-rays, K_λ is the product of the wavelength of the radiation in the constant of the device, the value of which it's value is constant 0.9. X-ray pattern of the $MgO/MgAl_2O_4$ nanoparticles is showed at Fig. 1a. The X-ray pattern of the $MgO/MgAl_2O_4$ nanoparticles show which the structure follows the hexagonal pattern and the crystal structure is fully formed in it. As shown in the presented pattern, the X-ray pattern obtained for $MgO/MgAl_2O_4$ NPs have a good conformity with the XRD pattern of the bulk structures. The results of the X-Ray Diffraction (XRD) spectroscopy analysis to quantify the elements in the sample are reported in Fig. 1b. The highest mass percentages of elements were Mg,O and Al respectively, which are the main elements of the composition. Elements such as N and Na impurities were also present in the composition, which can be related to CTAB and NaOH. In order to investigate the size range of the products, dynamic light scattering analysis was used.

DLS diagram of the $MgO/MgAl_2O_4$ NPs presented in Fig. 2a. Dn 10%: 10.19 nm, Dn 50%: 13.44 nm, Dn 90%: 18.58 nm were calculated. This indicates that the $MgO/MgAl_2O_4$ NPs were produced with a suitable and uniform size distribution. ThermoGravimetric (TG) analysis represents a curve for weight change as a function of temperature or time. Figs. 2b shows the TGA profile for the $MgO/MgAl_2O_4$ NPs. As can be seen the TG curve exhibits a double stage of decomposition for $MgO/MgAl_2O_4$ NPs, this type of the curve can be resulted when there is increment in weight for sample due to surface oxidation reactions that take place in a reacting atmosphere. It is anticipated which at the first water trapped in the structure is lost, then cross linking between MgO and $MgAl_2O_4$ and also Mg-O-Al are destroyed at 102°C, then at the higher temperatures about 245°C that more mass is lost, this can be related to the complete thermal decomposition of the nanocomposites [31].

To study the effect of solvent effect, precursor concentration, reaction conditions on the morphology of final products we used scanning electron microscopy. The results of scanning electron microscopy images for the $MgO/MgAl_2O_4$ NPs related to sample a:S_1, b:S_2, c:S_3 and d:S_4 under different synthesis conditions according to Table 1 are given in Figs. 3a, 3b, 3c and 3d, respectively. As shown in SEM images, by increasing of the temperature,

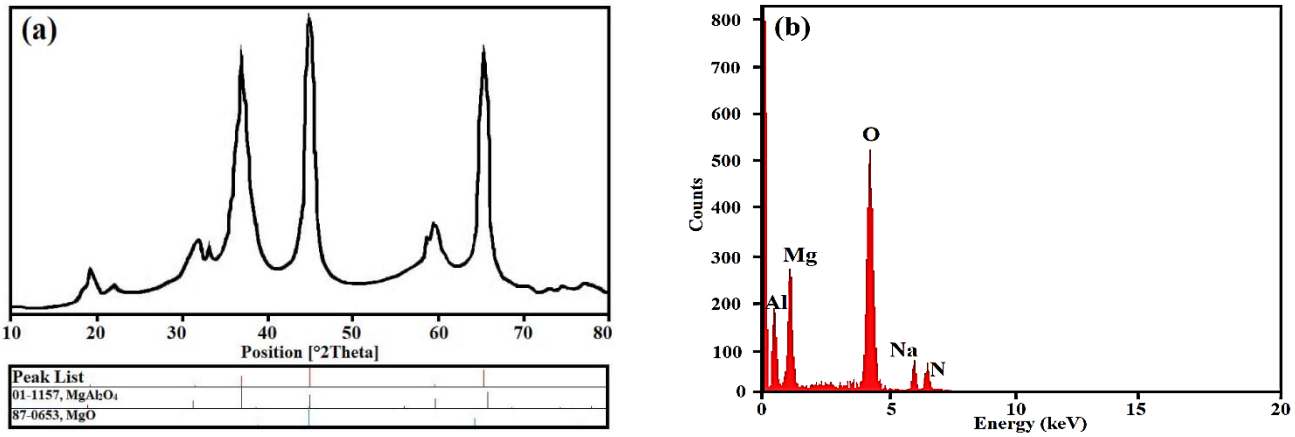

Fig. 1: X-ray diffraction pattern of $MgO/MgAl_2O_4$ NPs (a) and EDX analysis (b).

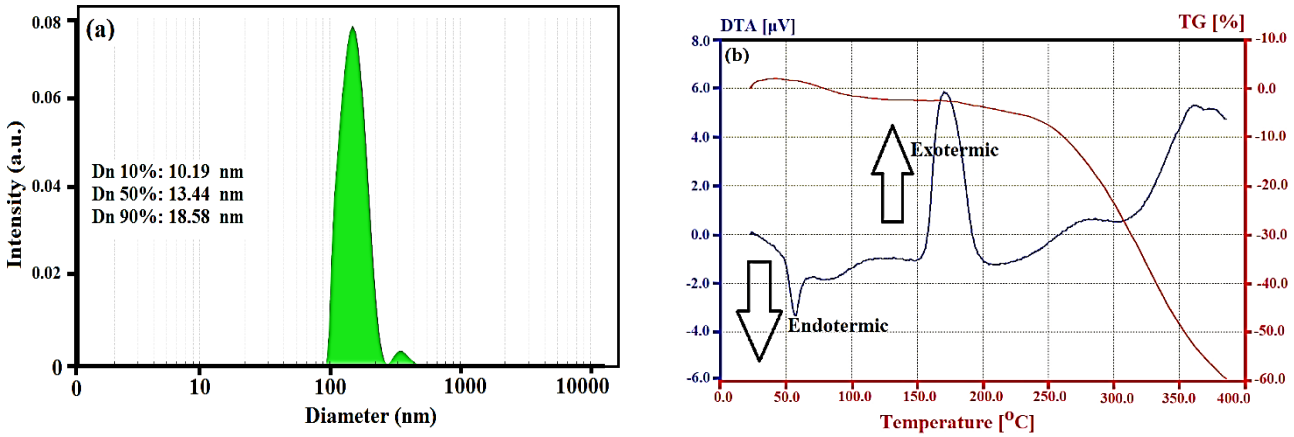

Fig. 2: DLS diagram (a) and TGA/DTA profile of the $MgO/MgAl_2O_4$ NPs.

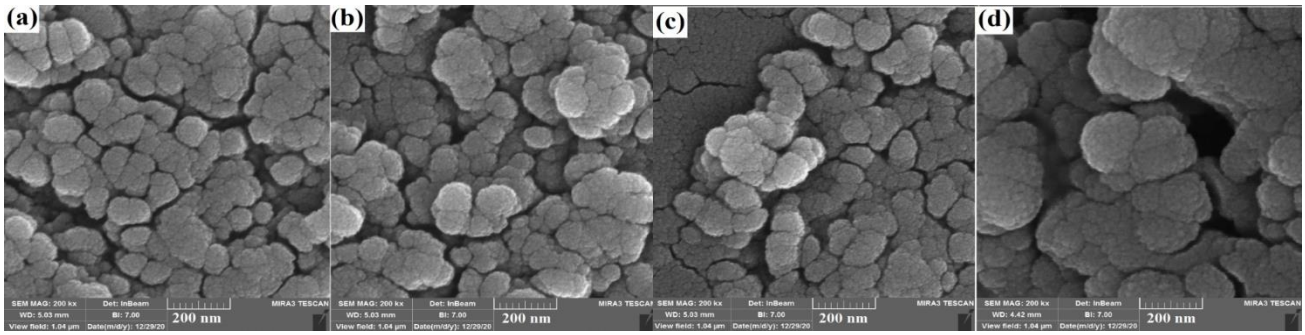

Fig. 3: SEM images of the $MgO/MgAl_2O_4$ NPs related to sample S_1 (a), S_2 (b) S_3 (c) and S_4 (d) respectively.

the particle size of the $MgO/MgAl_2O_4$ NPs remains constant and does not change much but in some areas, agglomeration are observed which this can be due to the active particle surface effect.

FT-IR results of the $MgO/MgAl_2O_4$ NPs were evaluated in the wavelength range of 500 cm^{-1} to 3500 cm^{-1}. The peaks appeared around 3500 cm^{-1} can be related to the H-O bonds which is probably related to the absorption of water on the surface of the $MgO/MgAl_2O_4$ NPs. The peaks at the range 1570 cm^{-1} can be related to the C-H bond in the CTAB. The peak observation in position 800 cm^{-1} for O-Al-O bonds after cross-linking between the MgO and $MgAl_2O_4$ [32]. The symmetric stretching bonds of O-Mg-O in $MgO/MgAl_2O_4$ NPs can be observed at about 650 cm^{-1}. The FT-IR spectrum of the as-synthesized $MgO/MgAl_2O_4$ NPs indicated in Figs. 4a [31]. In order to further study of

Table 2: The results of the MIC in the presence of $MgO/MgAl_2O_4$ NPs for 8 bacterial strains.

Concentration (µg/mL)	64	32	16	8	4	2	1	0.5	0.25
E.coli PTCC 1330	-	-	-	-	-	-	-	+	+
K.pneumoniae PTCC 1053	-	-	-	-	-	-	-	+	+
S.marsescens PTCC 1621	-	-	-	-	-	-	-	+	+
B. subtilis PTCC 1023	+	+	+	+	+	+	+	+	+
M. luteus PTCC 1110	+	+	+	+	+	+	+	+	+
S. aureus PTCC 1112	-	-	-	-	-	+	+	+	+
P. aeruginosa PTCC 1074	+	+	+	+	+	+	+	+	+
S. epidermidis PTCC.1114	-	+	+	+	+	+	+	+	+

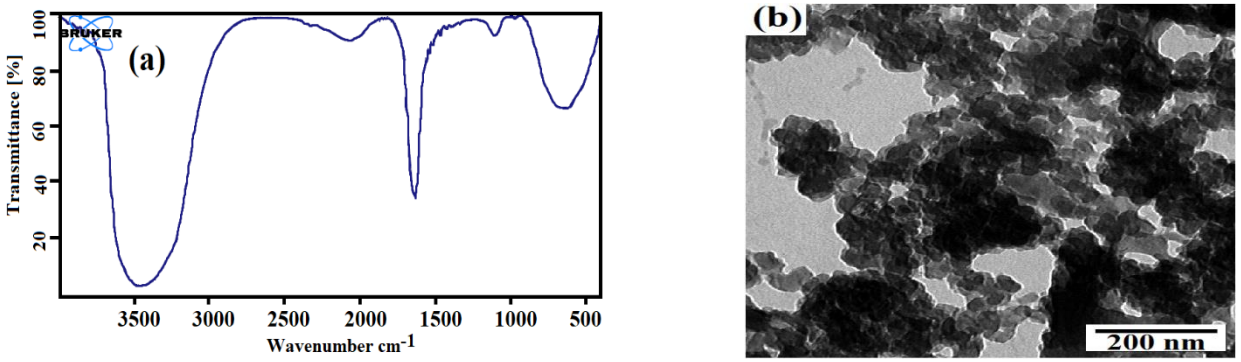

Fig. 4: The FT-IR spectrum of the $MgO/MgAl_2O_4$ NPs (a) and TEM image of the $MgO/MgAl_2O_4$ NPs (b).

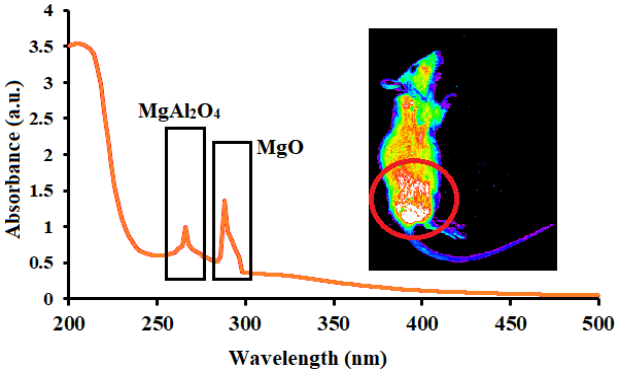

Fig. 5: The UV spectrum of the $MgO/MgAl_2O_4$ NPs and in vivo image of mice 2 min after of injection.

morphology, particle size distribution and surface properties transmission electron microscopy (TEM) analysis was performed. TEM image of the $MgO/MgAl_2O_4$ NPs demonstrated in Fig. 4b. The TEM image obtained has a good adjustment with the SEM image. In some areas, accumulations have been formed which can be due to increased surface activity in the $MgO/MgAl_2O_4$ NPs. According to TEM images spherical structures are approved and in some areas clusters of particles have formed.

Ultraviolet and Visible spectroscopy (UV-Vis) as an important analysis used in this study for the optical properties analysis. With the absorption of electromagnetic radiation, bonded electrons, or capacitance layer electrons in $MgO/MgAl_2O_4$ NPs are the most excited and become usually the most likely transition from the Highest Occupied Molecular Orbital (HOMO) to the Lowest Unoccupied Molecular Orbital (LUMO). The UV spectrum measurement for $MgO/MgAl_2O_4$ NPs is shown in Figs. 5. The results of the UV-Vis spectroscopy show that the first peak was observed at a wavelength between 260 and 270 nm which can be related to MgO nanoparticles [33, 34], and the maximum absorption was related to the wavelength of 282 nm. The redshift observed in the UV spectrum could be due to more existence of structural defects in MgO because of the presence of $MgAl_2O_4$. For the investigation of the optical properties 0.001 mg/mL $MgO/MgAl_2O_4$ NPs at 1:2 ratios of three times distilled water to ethanol injected to the rat tail (Balb/c male), 2 minutes after of injection in vivo image illustrated in Fig. 5. Anesthesia was done through 1:2 ratios of ketamine/xylazine. Male Balb/c weighing 150–200 g was fed with standard diet protocols and kept under

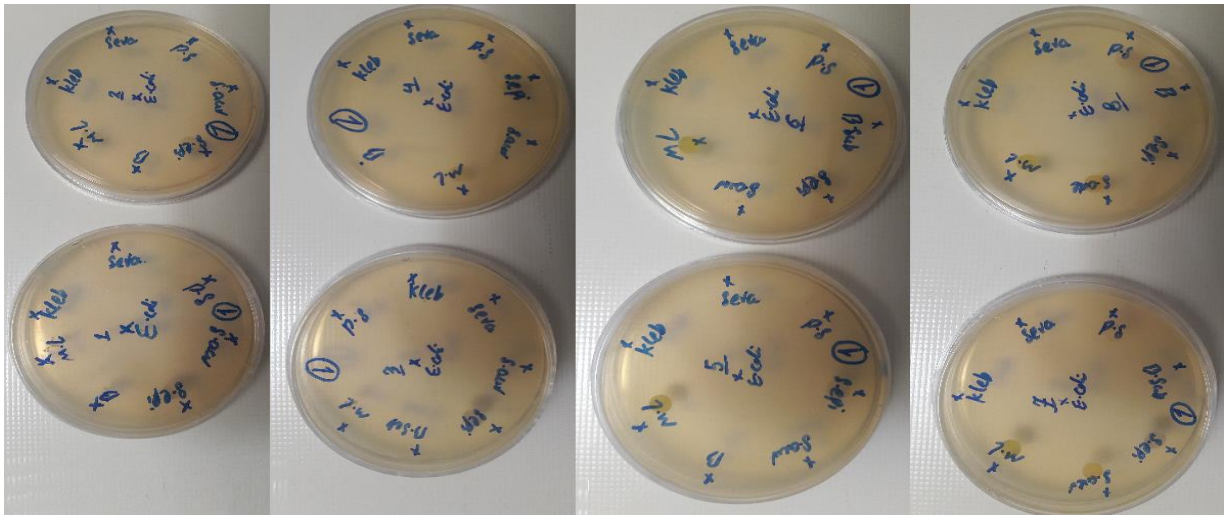

Fig. 6. The final concentrations for plates were achieved from respectively 0.25 µg/mL, 0.5 µg/mL, 1 µg/mL, 2 µg/mL, 4 µg/mL, 8 µg/mL, 16 µg/mL, 32 µg/mL, 64 µg/mL of an antimicrobial $MgO/MgAl_2O_4$ NPs (a-c).

2:12 h light/dark cycles, at 20°C and relative humidity of 25–30% according to the local ethical committee of the Kerman University of Medical Sciences. These results show that $MgO/MgAl_2O_4$ NPs with unique optical properties can be used as drug carriers and interceptors in living organisms.

To the investigation of antimicrobial effects of the as-synthesized $MgO/MgAl_2O_4$ NPs was used the MIC method. The results in Table 2 for the MIC in the presence of the $MgO/MgAl_2O_4$ NPs show the inhibitory effects of bacterial growth. The final concentrations for plates were achieved from 0.25 µg/mL, 0.5 µg/mL, 1 µg/mL, 2 µg/mL, 4 µg/mL, 8 µg/mL, 16 µg/mL, 32 µg/mLl, 64 µg/mL of an antimicrobial $MgO/MgAl_2O_4$ NPs respectively. The least growth inhibitory effects were observed on *E. coli*, *K.pneumoniae* and *S.marsescens* (0.5 µg/mL <MIC≤ 1 µg/mL). *S. aureus* was grown at concentrations less than equal to 4 µg/mL of the $MgO/MgAl_2O_4$ NPs (2 µg/mL < MIC≤4 µg/mL). *S. epidermidis* was also affected under the antimicrobial effects of the $MgO/MgAl_2O_4$ NPs (32 µg/mL <MIC ≤64 µg/mL). *Serachia marcenses* was also affected under the antimicrobial effects of the $MgO/MgAl_2O_4$ NPs (0.5 µg/mL <MIC≤1 µg/mL), Fig. 6.

CONCLUSIONS

In this study for the first time, $MgO/MgAl_2O_4$ NPs were synthesized with cost effective and eco-friendly assisted hydrothermal method. About the mechanism of antibacterial effects of this nanocomposites, three possible mechanisms are considered. In the case of aerobic bacteria, the effect of the $MgO/MgAl_2O_4$ NPs masking and preventing the penetration of oxygen into the bacteria can also be one of the possible mechanisms [35]. The final products, $MgO/MgAl_2O_4$ NPs, were characterized by EDX, XRD, SEM, DLS, TGA, TEM, UV spectrometer and FT-IR. *In vivo* observations of living organisms show that these structures can be used as anti-cancer drug carriers with unique optical properties.

Acknowledgments

Institute of Neuropharmacology, Kerman University of Medical Sciences, also Laboratory of Nanostructures and Nanodrugs Materials, Kerman, Iran. This study received ethical approval (98000408) and (IR.KMU.REC.1398.366.) from the local ethical committee of the Kerman University of Medical Sciences.

Received: Jan. 18, 2023 ; Accepted: Mar. 13, 2023

References

[1] Peters R.J., van Bemmel G., Herrera-Rivera Z., Helsper H.P., Marvin H.J., Weigel S., Tromp P.C., Oomen A.G., Rietveld A.G., Bouwmeester H., Characterization of Titanium Dioxide Nanoparticles in Food Products: Analytical Methods to Define Nanoparticles, *Journal of Agricultural and Food Chemistry*, **62(27):** 6285-6293 (2014).

[2] Lee S., Bi X., Reed R.B., Ranville J.F., Herckes P., Westerhoff P., Nanoparticle Size Detection Limits by Single Particle Icp-Ms for 40 Elements, *Environmental Science & Technology*, **48(17):** 10291-10300 (2014).
[3] Nandiyanto A.B.D., Okuyama K., Progress in Developing Spray-Drying Methods for the Production of Controlled Morphology Particles: From the Nanometer to Submicrometer Size Ranges, *Advanced Powder Technology*, **22(1):** 1-19 (2011).
[4] Ku K.H., Shin J.M., Yun H., Yi G.R., Jang S.G., Kim B.J., Multidimensional Design of Anisotropic Polymer Particles from Solvent-Evaporative Emulsion, *Advanced Functional Materials*, **28(42):** 1802961 (2018).
[5] Cheng X., Long D., Chen L., Jansen J.A., Leeuwenburgh S.C., Yang F., Electrophoretic Deposition of Silk Fibroin Coatings with Pre-Defined Architecture to Facilitate Precise Control over Drug Delivery, *Bioactive Materials*, **6(11):** 4243-4254 (2021).
[6] Avaz Seven S., Oguz O., Menceloglu Y.Z., Atilgan C., Tuning Interaction Parameters of Thermoplastic Polyurethanes in a Binary Solvent to Achieve Precise Control over Microphase Separation, *Journal of Chemical Information and Modeling*, **59(5):** 1946-1956 (2019).
[7] Baran G.R., Kiani M.F., Samuel S.P., "Healthcare and Biomedical Technology in the 21st Century: An Introduction for Non-Science Majors", Springer, (2013).
[8] Niu Y.B., Yin Y.X., Guo Y.G., Nonaqueous Sodium-Ion Full Cells: Status, Strategies, and Prospects, *Small*, **15(32):** 1900233 (2019).
[9] Zhai J., Fong C., Tran N., Drummond C.J., Non-Lamellar Lyotropic Liquid Crystalline Lipid Nanoparticles for the Next Generation of Nanomedicine, *ACS Nano*, **13(6):** 6178-6206 (2019).
[10] Saeedi M., Eslamifar M., Khezri K., Dizaj S.M., Applications of Nanotechnology in Drug Delivery to the Central Nervous System, *Biomedicine & Pharmacotherapy*, **111:** 666-675 (2019).
[11] Gupta N., Rai D.B., Jangid A.K., Kulhari H., Use of Nanotechnology in Antimicrobial Therapy, *Methods in Microbiology*, **46:** 143-172 (2019).
[12] Kamran U., Bhatti H.N., Iqbal M., Jamil S., Zahid M., Biogenic Synthesis, Characterization and Investigation of Photocatalytic and Antimicrobial Activity of Manganese Nanoparticles Synthesized from Cinnamomum Verum Bark Extract, *Journal of Molecular Structure*, **1179:** 532-539 (2019).
[13] Cheng A.V., Wuest W.M., Signed, Sealed, Delivered: Conjugate and Prodrug Strategies as Targeted Delivery Vectors for Antibiotics, *ACS Infectious Diseases*, **5(6):** 816-828 (2019).
[14] Kraft J.C., Freeling J.P., Wang Z., Ho R.J., Emerging Research and Clinical Development Trends of Liposome and Lipid Nanoparticle Drug Delivery Systems, *Journal of Pharmaceutical Sciences*, **103(1):** 29-52 (2014).
[15] Ezrahi S., Aserin A., Garti N., Basic Principles of Drug Delivery Systems–the Case of Paclitaxel, *Advances in Colloid and Interface Science*, **263:** 95-130 (2019).
[16] Herrmann J., Vascular Toxic Effects of Cancer Therapies, *Nature Reviews Cardiology*, **17(8):** 503-522 (2020).
[17] Sulaiman G.M., Waheeb H.M., Jabir M.S., Khazaal S.H., Dewir Y.H., Naidoo Y., Hesperidin Loaded on Gold Nanoparticles as a Drug Delivery System for a Successful Biocompatible, Anti-Cancer, Anti-Inflammatory and Phagocytosis Inducer Model, *Scientific Reports*, **10(1):** 1-16 (2020).
[18] Ebert A.D., Svendsen C.N., Human Stem Cells and Drug Screening: Opportunities and Challenges, *Nature Reviews Drug Discovery*, **9(5):** 367-372 (2010).
[19] Arias L.S., Pessan J.P., Vieira A.P.M., Lima T.M.T.d., Delbem A.C.B., Monteiro D.R., Iron Oxide Nanoparticles for Biomedical Applications: A Perspective on Synthesis, Drugs, Antimicrobial Activity, and Toxicity, *Antibiotics*, **7(2):** 46 (2018).
[20] Mansur A.A., Carvalho S.M., Lobato Z.I.I., Leite M.d.F., Cunha Jr A.d.S., Mansur H.S., Design and Development of Polysaccharide-Doxorubicin-Peptide Bioconjugates for Dual Synergistic Effects of Integrin-Targeted and Cell-Penetrating Peptides for Cancer Chemotherapy, *Bioconjugate Chemistry*, **29(6):** 1973-2000 (2018).
[21] Rastogi A., Zivcak M., Sytar O., Kalaji H.M., He X., Mbarki S., Brestic M., Impact of Metal and Metal Oxide Nanoparticles on Plant: A Critical Review, *Frontiers in Chemistry*, **5:** 78 (2017).

[22] Mallakpour S., Madani M., A Review of Current Coupling Agents for Modification of Metal Oxide Nanoparticles, *Progress in Organic Coatings*, **86:** 194-207 (2015).

[23] Sengul A.B., Asmatulu E., Toxicity of Metal and Metal Oxide Nanoparticles: A Review, *Environmental Chemistry Letters* **18:** 1659-1683 (2020).

[24] Agarwal H., Nakara A., Shanmugam V.K., Anti-Inflammatory Mechanism of Various Metal and Metal Oxide Nanoparticles Synthesized Using Plant Extracts: A Review, *Biomedicine & Pharmacotherapy*, **109:** 2561-2572 (2019).

[25] Yu Z., Gunn L., Wall P., Fanning S., Antimicrobial Resistance and Its Association with Tolerance to Heavy Metals in Agriculture Production, *Food Microbiology*, **64:** 23-32 (2017).

[26] Bush K., Page M.G., What We May Expect from Novel Antibacterial Agents in the Pipeline with Respect to Resistance and Pharmacodynamic Principles, *Journal of Pharmacokinetics and Pharmacodynamics*, **44(2):** 113-132 (2017).

[27] Kumar H., Bhardwaj K., Kuča K., Kalia A., Nepovimova E., Verma R., Kumar D., Flower-Based Green Synthesis of Metallic Nanoparticles: Applications Beyond Fragrance, *Nanomaterials*, **10(4):** 766 (2020).

[28] Fernández-García M., Rodriguez J.A., Metal Oxide Nanoparticles, "Encyclopedia of inorganic And Bioinorganic Chemistry" (2011).

[29] Jeng H.A., Swanson J., Toxicity of Metal Oxide Nanoparticles in Mammalian Cells, *Journal of Environmental Science and Health Part A*, **41(12):** 2699-2711 (2006).

[30] Umamah C., Pratapa S., Andi H.J., The Effect of Mg-Al Wt% for Phase Formation of Spinel $MgAl_2O_4$ Produced by Metal Dissolved Method, *Jurnal Neutrino: Jurnal Fisika dan Aplikasinya*, **12(1):** 21-29 (2019).

[31] Vahid B.R., Haghighi M., Urea-Nitrate Combustion Synthesis of $MgO/MgAl_2O_4$ Nanocatalyst Used in Biodiesel Production from Sunflower Oil: Influence of Fuel Ratio on Catalytic Properties and Performance, *Energy Conversion and Management*, **126:** 362-372 (2016).

[32] Ewais E.M., El-Amir A.A., Besisa D.H., Esmat M., El-Anadouli B.E., Synthesis of Nanocrystalline $MgO/MgAl_2O_4$ Spinel Powders from Industrial Wastes, *Journal of Alloys and Compounds*, **691:** 822-833 (2017).

[33] Nemade K., Waghuley S., Synthesis of MgO Nanoparticles by Solvent Mixed Spray Pyrolysis Technique for Optical Investigation, *International Journal of Metals*, **2014:** (2014).

[34] Varshney D., Dwivedi S., On the Synthesis, Structural, Optical and Magnetic Properties of Nano-Size Zn–Mgo, *Superlattices and Microstructures*, **85:** 886-893 (2015).

[35] Aasim M., Foto E., Sameeullah M., "Nanoparticles for Sustainable Bioenergy and Biofuel Production", Springer, 23-60 (2020).